PHYSICAL REVIEW B **72**, 214414 (2005)

First-principles study of ultrathin magnetic Mn films on W surfaces. II. Surface diffusion

S. Dennler* and J. Hafner
Institut für Materialphysik and Center for Computational Materials Science, Universität Wien, Sensengasse 8, A-1090 Wien, Austria

(Received 22 July 2005; revised manuscript received 30 September 2005; published 9 December 2005)

The atomic diffusion in the first stages of the growth of ultrathin Mn films deposed on W substrates has been investigated in the framework of the density functional theory. The most stable adsorption sites and the activation energy barriers associated to the elementary dynamical processes occurring during the diffusion of Mn adatoms on clean and Mn-covered W(100) and W(110) surfaces have been determined. The Mn surface diffusion is governed by the hopping from stable adsorption sites to nearest-neighbor positions while exchange with underlying surface atoms is rather unlikely due to much higher energy barriers. The comparison between magnetic and nonmagnetic calculations reveals the strong influence of magnetism both on adsorption sites and diffusion properties. The pseudomorphic growth of the first layers is stabilized through the magnetic interaction between adlayer and substrate atoms. Magnetism generally induces a remarkable decrease of the diffusion barriers, but an increase can also be observed in some cases for antiferromagnetic Mn films deposed on the W(110) surface, due to magnetic frustration effects.

DOI: 10.1103/PhysRevB.72.214414 PACS number(s): 75.70.Ak, 68.43.Bc, 68.35.Fx, 68.43.Jk

I. INTRODUCTION

The heteroepitaxial growth of ultrathin films of ferromagnetic metals on nonmagnetic substrates, with the aim of tailoring their structural and magnetic properties, has been a very active field of research during the past two decades. However, much less effort has been spent on the preparation and investigation of antiferromagnetic films. The growth of ultrathin films of manganese (Mn) could prove to be particularly rewarding, because the existence of five different crystalline modifications with different types of magnetic ordering,[1,2] and the observation of a strong surface-induced enhancement of the magnetic moments[3] suggests a rich scenario of magnetic effects in Mn films. Recently, Bode *et al.*[4–6] have demonstrated that highly strained films of body-centered-tetragonal δ-Mn can be grown on W(110) surfaces up to a local thickness of three atomic layers. The formation of pseudomorphic Mn/W(100) films has been reported by Tian *et al.*[7] In our preceding paper (which will hereafter be referred to as paper I),[8] the structural and magnetic properties of ultrathin Mn films deposed on W substrates have been explored within the framework of density functional theory. This study which has focused on compact films has demonstrated that pseudomorphically grown Mn/W(110) and Mn/W(100) films up to three layers are thermodynamically stable, in good agreement with experiments. Their complex magnetic magnetic properties have been determined in a fully first-principles approach. Mn/W(110) films show in-plane $c(2\times2)$ antiferromagnetism for a film thickness of up to 3 monolayers, while—very surprisingly—Mn/W(100) are found to be ferromagnetic up to 2 monolayers. For thicker films, layered antiferromagnetism is favored on both substrates. It has been shown that the stability of the pseudomorphic films, despite of a large nominal mismatch, depends strongly on magnetic effects, the strong surface-induced enhancement of magnetism causes a magnetovolume expansion significantly reducing the mismatch at the interface.

However, even if the calculations establish the thermodynamic stability of heteroepitaxial films, their morphology will be strongly influenced by the diffusion of the atoms forming the growing film. The STM images of Bode *et al.*[4–6] revealed that already the first Mn monolayer grows anisotropically along the [001] direction of the substrate, and that the anisotropy becomes distinctly more pronounced for the second monolayer. Beyond a thickness of three monolayers, island growth is reported. All this is in striking contrast to the growth mode observed for Fe/W(110) films. In addition, although Mn has an even lower surface free energy[9] than Fe and hence the formation of a compact overlayer should be even more favorable, Mn forms no wetting overlayer on W(110) as Fe does.

Therefore, to achieve a better insight in the growth mechanism of the films, the investigation of atomic diffusion in these systems is particularly worthwhile. The diffusion of Fe on W surfaces and on Fe/W films has recently been studied by Spišák and Hafner[10] using *ab initio* density-functional theory (DFT). The results of these studies are remarkable in several respects. (i) Modest activation energies for hopping diffusion and very high barriers for exchange diffusion favor the formation of smooth Fe/W films. (ii) For Fe diffusion on W(110), the calculated activation energies are in very good agreement with experiment—this validates DFT calculations of diffusion constants. (iii) For Fe diffusion on Fe/W films, magnetic effects play a very important role in adatom diffusion. Magnetic ordering considerably reduces the corrugation of the potential-energy surface, so that diffusion at low temperature on a magnetically ordered film can be faster than diffusion at high temperature on a nonmagnetic film. In the present work our studies of the structural and magnetic properties of Mn films on W(100) and W(110) are extended to the investigation of diffusion processes of Mn atoms on clean W surfaces and on Mn/W films, and of vacancies in these films. In the following, after a short presentation of our specific computational approach (Sec. II) we present in Secs. III and IV our results for the elementary dynamical processes involved in Mn surface diffusion on clean W surfaces and on Mn/W films, respectively. Finally, Sec. V summarizes our results and points to future developments.

II. COMPUTATIONAL DETAILS

Our calculations were carried out within the density functional framework (DFT) using the Vienna *ab initio* simulation package (VASP)[11,12] implementing the projector-augmented wave (PAW) method.[13,14] A general presentation of our computational framework has already been given in paper I, here we only focus on the specific parameters we adjusted to study the dynamical processes in which we are interested in this paper.

Basically, an adatom can move from a stable site to a vacant neighboring one by two main processes, (i) hopping between two neighboring adsorption sites, (ii) exchange with an atom of the underlying layer which is the pushed out at the surface.[15,16] Detailed comparative studies of self-diffusion on metallic surfaces via hopping and exchange mechanism have demonstrated that the transition state for atomic exchange creates a long-ranged strain field.[17,18] Hence relatively large surface cells must be used to achieve converged results for the activation energy for exchange diffusion, convergence of the barrier for hopping diffusion is always much faster. To account for the influence of the long-ranged strain fields, we have used sufficiently large models with 4×4 and 3×3 surface cells for studying adatom adsorption and migration on W(100) and W(110) surfaces, respectively. Therefore, to maintain tractable computation times the slab thickness was reduced to four substrate layers of which two were kept fixed in bulklike positions with the calculated W bulk lattice constant. Still, on the basis of the earlier studies of surface diffusion, we estimate that the barrier height for exchange diffusion calculated with these surface cells is larger by about 0.1 eV than the true activation energy.[17] However, we find that the differences in the barrier heights between hopping and exchange processes are always much large than this remaining uncertainty so that our choice represents an acceptable compromise.

Like previously, the geometric relaxation was performed with a quasi-Newton algorithm using the exact Hellmann-Feynman forces, with a criterion for stopping the structural optimization of 0.01 eV/Å. Our *ab initio* framework allowed us to compute the energy barrier associated with each of the events which is defined by the energy difference between the initial stable adsorbed state and the saddle point (transition state) separating the initial state basin to that of the final state. The values of the barriers were determined by comparing initial and transition states directly, if the latter had a high structural and magnetic symmetry, or the transition state was determined by means of the nudged elastic band (NEB) method.[19] In the NEB method, a set of intermediate states along the diffusion path is constructed and relaxed in the hyperspace perpendicular to the path.

Unless stated explicitly, the calculations take into account magnetism through a spin-polarized DFT approach. Local magnetic moments were calculated by integrating the magnetization densities within atom-centered spheres with radii of 1.373Å, corresponding to touching spheres in bulk tungsten. Moreover, since the magnetic ordering temperature is not known for these systems and may be high enough to be relevant, we performed in each case magnetic and nonmagnetic calculations. Their comparison gives a good estimation of the magnetic contribution to the diffusion mechanisms.

III. DIFFUSION OF Mn ON THE CLEAN W SURFACES

We begin our discussion by the diffusion of Mn adatoms on the clean W(100) and W(110) surfaces. The clean tungsten surfaces have already been described in paper I.

A. Adsorption sites

1. W(100) surface

It is well known that the clean W(100) surface undergoes a $(\sqrt{2}\times\sqrt{2})R45°$ reconstruction,[20] which is well reproduced by DFT calculations. On the reconstructed W(100) surface where the nearest-neighbor squares are deformed to a deltoid with an acute angle of 77.8° (see Fig. 1 in paper I) the most favorable adsorption site for a Mn atom is the fourfold hollow site, the adatom located 1.31 Å above the surface induces a modification of the local surface geometry, which locally leads to the almost complete removal of the surface reconstruction. The square geometry characterizing the (100) surface is locally almost recovered with angles of about 85°. The bridge positions on the long and short edges of the deltoid on the reconstructed W(100) surface are significantly less stable by 1.06 and 1.16 eV, respectively.

These results are a first hint that a pseudomorphic growth of Mn on W(100) can be achieved, at least at a local scale. For the sake of simplicity we will consider in the following the nonreconstructed relaxed W substrate [Fig. 1(a)]. In this case, the Mn atom also lies in the fourfold hollow at 1.43 Å above the surface. The bridge position [Fig. 1(c)] represents a transition state for adatom diffusion with an energy increased by 1.23 eV compared to the hollow site.

2. W(110) surface

The case of W(110) is simpler since this surface does not exhibit any surface reconstruction. The Mn adatom prefers stay in the long bridge between two W surface atoms [oriented along the $\langle 100\rangle$ direction, Fig. 1(b)], at about 1.84 Å above the surface. The short bridge site [along the $\langle 110\rangle$ direction, Fig. 1(d)] is less stable by 0.41 eV (the adatom lies 1.99 Å above the surface), while the pseudothreefold hollow turns out to be unstable.

3. Magnetic effects

For both (100) and (110) substrates, the Mn adatom retains a quite large magnetic moment of $\mu_{100}=1.98\mu_B$ and $\mu_{110}=2.73\mu_B$, respectively. Note that μ_{110} is higher due to the reduced atomic coordination of Mn in the bridge site. Magnetism has moreover a substantial stabilizing effect as the magnetic solution is more stable by 85 meV and 131 meV than the nonmagnetic Mn/W(100) and Mn/W(110) configurations. As illustrated in Fig. 1, small antiparallel magnetic moments are induced on neighboring W atoms. They amount to about $-0.14\mu_B$/atom for the four W atoms

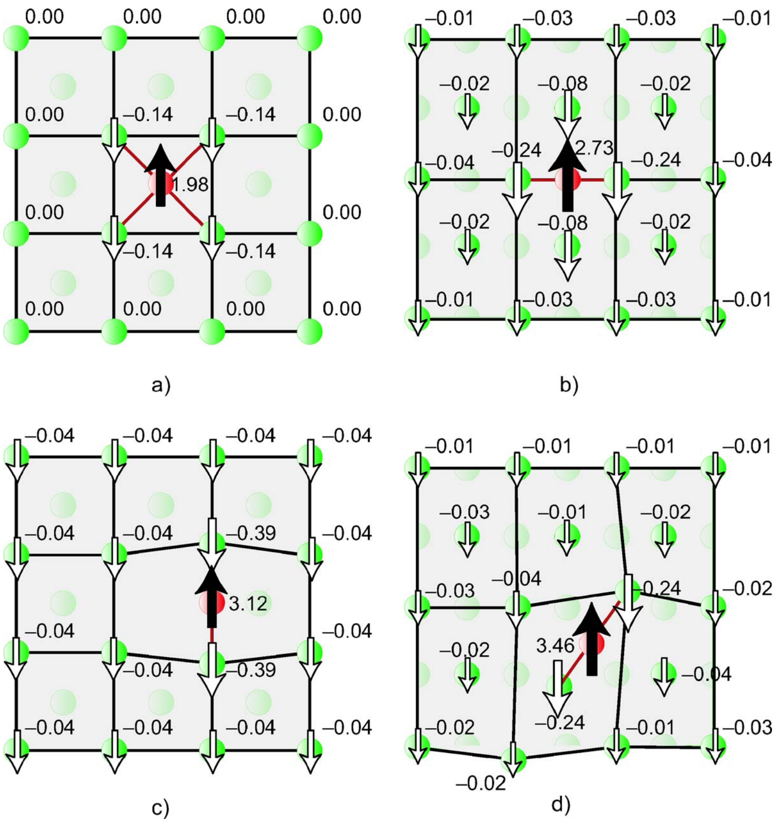

FIG. 1. (Color online) Local magnetic moments for an isolated Mn atom adsorbed on the clean nonreconstructed relaxed W(100) and W(110) surfaces. Top pictures illustrate the most stable adsorption sites, while bottom pictures represent the transition states for the hopping processes into the nearest vacant adsorption sites (cf. Fig. 2), showing the geometric and magnetic distortions of the lattice.

surrounding the Mn atom on W(100), and already vanish for the next-nearest neighbors. For Mn/W(110) the induced moments extend slightly further due to the more compact substrate. Their value for the two W atoms forming the bridge where Mn is adsorbed, $-0.24\mu_B/\text{atom}$, is higher due to the reduced coordination.

B. Diffusion barriers

The corresponding energy barriers for the diffusion of Mn adatoms on W(100) and W(110) are summarized in Fig. 2, for magnetic and nonmagnetic calculations. We first consider the magnetic calculations.

To move to a next-neighboring vacant fourfold hollow on the ideal relaxed W(100) the Mn adatom must jump through a bridge position, leading to a hopping barrier of 1.23 eV. On the reconstructed W(100) surface, the barriers for the hopping over the long and short bridges, 1.06 and 1.16 eV, respectively, are slightly lower and very close, which shows no significant anisotropy in the Mn diffusion and is a further clue validating our choice to model the actual W(100) surface with the nonreconstructed one. For Fe on the reconstructed W(100) surfaces, Spišák and Hafner[10] calculated barriers for hopping diffusion of 1.2 eV and 1.3 eV, respectively.

Exchange diffusion of an impurity atom is a two-step process, in the first step, the adatom is incorporated in the surface, forming a surface impurity and a substrate atom is pushed out to the surface, a second exchange process can bring the impurity back into an adatom position. The exchange process of a Mn adatom with one of the neighboring W atoms of the substrate is highly improbable due to a high barrier of 2.02 eV. However, the final configuration with a Mn impurity in the surface and an ejected W atom has an energy lower by 92 meV than the Mn adatom. Slightly higher barriers for both hopping and exchange diffusion have been found for Fe on W(100).[10]

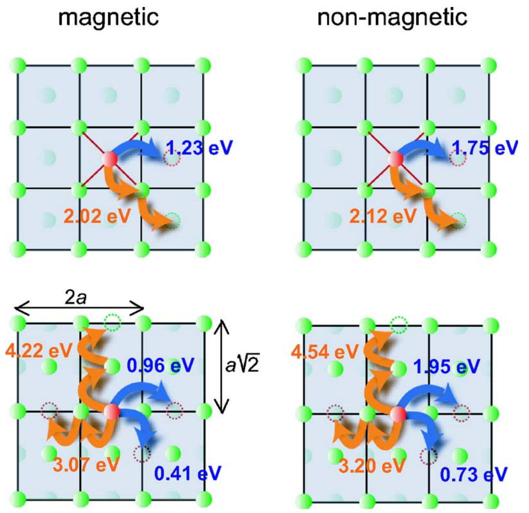

FIG. 2. (Color online) Energetic barriers (in eV) involved in the diffusion of isolated Mn atoms adsorbed on the clean W(100) (top) and W(110) (bottom) substrates, as obtained in magnetic (left-hand side) or nonmagnetic (right-hand side) calculations. Dark arrows depict hopping processes, lighter arrows diffusion via atomic exchange processes.

The diffusion on the W(110) follows a similar picture. To move from the most stable adsorption site, a long bridge site between two surface atoms, to a nearest vacant one, the Mn adatom must jump into another bridge position along the ⟨111⟩ direction. This hopping process has an activation energy of only 0.41 eV, much lower than that of Mn/W(100), 1.23 eV/atom, due to the higher density of the (110) surface which reduces the corrugation of the potential-energy surface for the Mn adatom. The hopping process through a transition state on top of the first-neighboring atom has also a low barrier of 0.96 eV. Reciprocally, the exchange processes with a substrate atom are even more unfavored than on W(100) and have much higher energy barriers of 3.07 and 4.22 eV for the exchange along the ⟨100⟩ and ⟨110⟩ directions, respectively. The difference between the two exchange barriers arises from the larger distance between the substrate atoms along the ⟨100⟩ direction which makes an exchange process easier compared to the more dense ⟨110⟩ direction. The exchange process on the W(110) surface requires not only a high activation energy, it is also strongly endothermic, the final-state configurations of the exchange process with the Mn incorporated in the surface and a W adatom in a neighboring bridge position have an energy higher by 0.89 eV and 1.32 eV, for exchange processes along the ⟨100⟩ and ⟨110⟩, respectively. Interestingly, in the final state for the former process, the Mn atom incorporated in the W surface loses completely its magnetic moment, while in the latter case it retains a large moment of $3.08\mu_B$.

Our calculations thus demonstrate that the predominant Mn diffusion mechanism on clean W surfaces is the hopping from a stable adsorption site to the next vacant one, while the exchange with a substrate atom is highly disfavored. This originates in the particularly strong binding between the W atoms which makes the W surfaces a good choice to obtain remarkably smooth adsorbed films without any significant interdiffusion at the interface.

From the magnetic point of view, it is important to note that in all configurations, the W substrate (which is nonmagnetic in the adsorbate-free state) becomes antiferromagnetically polarized around the Mn adatom over a few nearest-neighboring atoms, the magnetization amplitude depending on the local coordination. In their transition states for hopping diffusion on the (100) and (110) surfaces, the magnetic moment of the Mn adatoms is enhanced by $1.14\mu_B$ and $0.73\mu_B$, respectively. If magnetism is not taken into account, much higher activation energies are generally found as illustrated in Fig. 2. The enhanced values for the diffusion barriers originate from the need to quench a larger Mn moment in the transition state. The result that magnetism favors diffusion is certainly remarkable—it will be even more important for self-diffusion of atoms on a thin magnetic film.

IV. DIFFUSION OF Mn ON 1 ML THICK Mn/W FILMS

In this section we consider the diffusion of Mn adatoms once the W substrate has been covered by a Mn layer. In this case, magnetism is expected to play a large role since in paper I we have shown that thin complete Mn films exhibit a high-spin magnetism with moments reaching about $3.5\mu_B$.

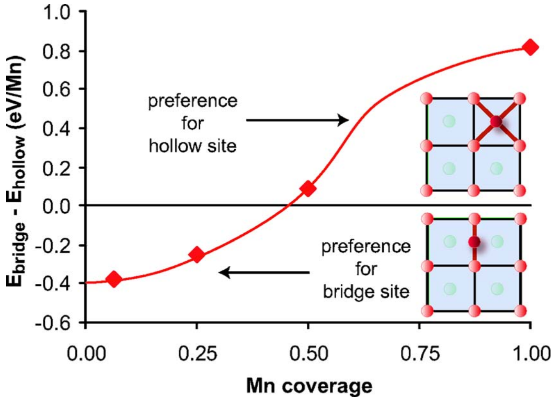

FIG. 3. (Color online) Energy difference between the bridge and hollow adsorption sites of Mn atoms adsorbed on a $Mn_1/W(100)$ substrate as a function of the Mn coverage, in nonmagnetic calculations. The line is a guide to the eye.

A. Diffusion of Mn on Mn/W(100) films

1. Adsorption sites

We address the case of the diffusion of Mn adatoms on a nonmagnetic Mn layer adsorbed on W(100) first. Our calculations presented in Fig. 3 demonstrate a strong dependence of the preferred adsorption site on the Mn coverage in the second layer. Very surprisingly, it turns out indeed that at low coverage (for coverages inferior to about 0.5 ML) the Mn atoms adsorb preferentially at the bridge sites; for an isolated adatom (which lies about 0.97 Å above the first Mn layer), the bridge is more stable by about 0.4 eV compared to the fourfold hollow. This is in contrast to the usual expectations that metal atoms should adsorb at the highest coordinated sites, but completely analogous to a partially Fe-covered Fe/W(100) film.[10] On the other hand, at large coverage when Mn–Mn interactions increase, the fourfold hollow site becomes favored. In this hollow configuration which is more stable by about 0.8 eV than the bridge site, an isolated Mn adatom is located about 0.88 Å above the Mn plane. This exceptionally low Mn–Mn interlayer distance corresponds to a large tetragonal distortion and a very large surface strain.

However, in paper I we have demonstrated that the magnetic ground state on a Mn monolayer on W(100) is ferromagnetic (FM). In this case, the fourfold hollow site is preferred at any coverage. A Mn adatom adsorbed on the 1 ML Mn/W(100) film is located 1.26 Å above the surface, i.e., substantially higher than in nonmagnetic calculations. As shown in Fig. 4(a), the Mn adatom exhibits a magnetic moment of $3.74\mu_B$ coupled ferromagnetically with the nearest-neighbor Mn atoms in the underlying film. The Mn adatom leads to a decrease of the magnetic moments on the surrounding atoms in the film relative to the value of $3.26\mu_B$ on a clean film. At a full 2 ML coverage, the Mn–Mn interlayer distance increases to 1.49Å, and the Mn moments in the surface layer to $3.87\mu_B$, while the moments in the Mn interface layer are reduced to a value close to the moment in bulk δ-Mn. Mn–Mn coupling remains ferromagnetic (for details, see paper I).

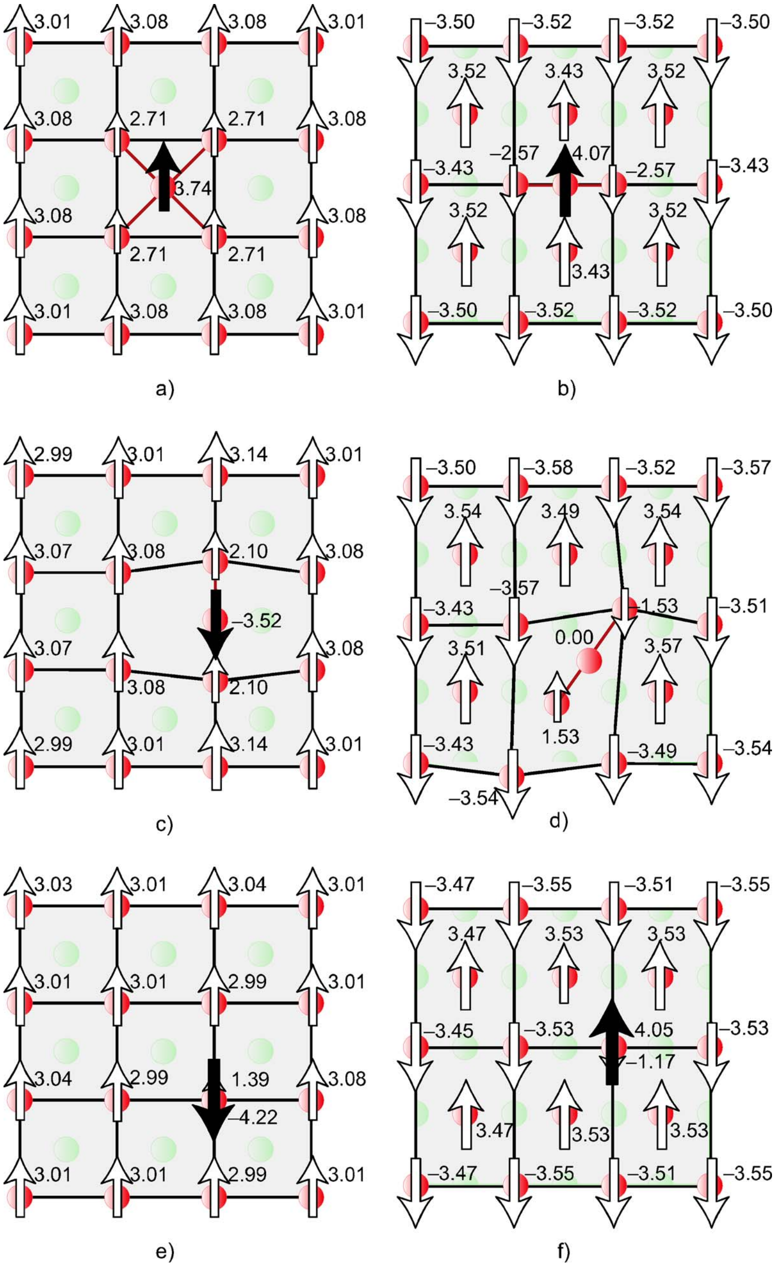

FIG. 4. (Color online) Local magnetic moments for an isolated Mn atom adsorbed on a 1 ML thick Mn film on W(100) (left-hand side) and W(110) (right-hand side). Top pictures illustrate the most stable adsorption sites, while bottom pictures represent the transition states for the hopping processes into the nearest vacant sites (cf. Figs. 5 and 9), showing the geometric and magnetic distortions of the lattice.

2. Diffusion barriers

The calculated barriers for the hopping and exchange diffusion on ferromagnetic and on nonmagnetic Mn/W(100) films are presented in Fig. 5.

For hopping diffusion the surprising result is that in the transition state (in the bridge position), the preferred orientation of the magnetic moment of the diffusing adatom is antiparallel to the Mn film [see Fig. 4(c)]. Hence diffusion is coupled to a transient spin reorientation of the adatom. To get more information on the influence of the magnetism of the adatom on the potential-energy profile for diffusion, we have performed NEB calculations for two different spin orientations of the adatom, see Fig. 6. In the hollow position, the AF orientation of the adatom is disfavored by 0.12 eV/atom relative to the FM configuration. However, the potential-energy profile is much flatter for an AF adatom. If the dif-

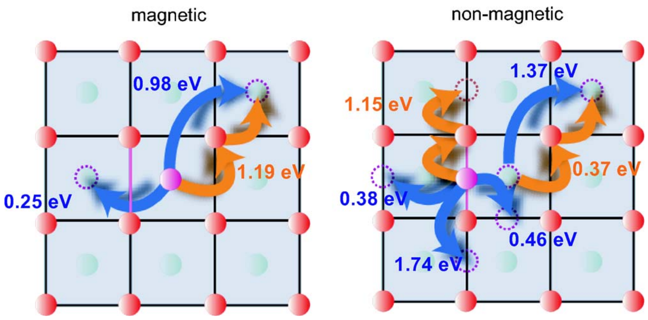

FIG. 5. (Color online) Energy barriers (in eV) involved in the diffusion of a Mn atom adsorbed on a 1 ML Mn/W(100) film, as obtained in magnetic (left-hand side) or nonmagnetic (right-hand side) calculations.

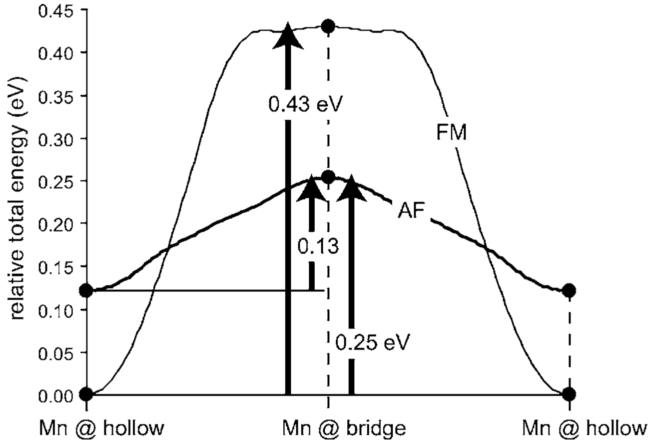

FIG. 6. Potential-energy profile for hopping diffusion of a Mn adatom on a 1 ML thick Mn/W(100) film, calculated for parallel (FM) and antiparallel (AF) orientation of the magnetic moment of the adatom relative to the moments in the FM Mn layer. Compare with text.

fusing atom does not change the orientation of its magnetic moment, we calculate a barrier of 0.43 eV, if a spin-reorientation is admitted, the barrier is reduced to 0.25 eV. Of course, the spin-reorientation itself could be hindered by a barrier, if a perpendicular orientation of the moment of the adatom relative to the substrate costs much energy. However, this could be determined only by a noncollinear calculation including spin-orbit coupling to account for the influence of the magnetic anisotropy—but this is definitely beyond the scope of the present work. The hopping barrier of 0.25 eV for nearest-neighbor jumps including spin reorientation should be considered as a lower limit, while the barrier of 0.43 eV calculated with a fixed FM coupling represents an upper limit. For second-neighbor hopping across a top position we find a minimal barrier of 0.98 eV, again for a transition state with an antiferromagnetic moment on the adatom [see Fig. 4(e)]. Diffusion via an exchange process has a barrier of 1.19 eV.

For Mn adatoms on a nonmagnetic 1 ML Mn/W(100) film the situation is very different, see Fig. 5. The equilibrium adsorption site is now the bridge position. Nearest-neighbor hopping along the ⟨111⟩ direction has an activation energy of 0.46 eV, hopping into a next-nearest-neighbor bridge site across a hollow has even a lower barrier of 0.38 eV, hopping across a top site leads to a much higher barrier of 1.74 eV, which is even higher than the barrier for exchange diffusion. If the adatom occupies the less favorable hollow site, exchange diffusion has an exceptionally low barrier of 0.37 eV—but this is a somewhat academic constrained scenario, as the adatom displaced from the hollow would certainly approach the equilibrium bridge site. Also the adatom position in the hollow is stable only at coverages higher than 0.5 ML, and at these coverages, the barriers are strongly influenced by lateral adatom interactions.

Hence similar conclusions as for diffusion on clean W surfaces can be drawn, (i) hopping is the dominant process for Mn diffusion with a very low barrier between 0.25 eV and ~0.4 eV, (ii) all barriers (and in particular those for exchange processes) appear to be significantly reduced with respect to those calculated for the clean W surfaces, and (iii) magnetic ordering leads to a lowering of the activation barriers for both exchange and hopping events. The reduced barrier height compared to the clean W substrate is explained by the moderate strength of the Mn–Mn bonding compared to the Mn-W and W–W ones. Consequently, exchanging the Mn adatom with a Mn surface one has a decreased energy cost since it does not require breaking strong W–W bonds, and the hopping of a Mn adatom is also easier since it feels a smaller friction. The influence of magnetism on the diffusion process requires some comments, the calculations reported here refer to nonmagnetic Mn/W(100) films, paramagnetic Mn films at temperatures above the Curie temperatures have disordered local moments. Hence at temperatures not too far above T_C local adatom configurations and diffusion barriers will be influenced by magnetic fluctuations.

Again a comparison with Fe/W(100) is instructive, the antiferromagnetic element Mn forms a FM monolayer on W(100), while the ferromagnetic element Fe forms an AF monolayer[10]—in both cases the change of the magnetic ground state compared to the bulk is caused by the strong adsorbate-substrate hybridization across the interface. Hence the results for Mn and Fe diffusion are immediately comparable only in the nonmagnetic case, here the hopping barriers are identical within the computational accuracy, while exchange diffusion of Fe on Fe/W(100) has a significantly lower barrier of 0.7 eV, compared to 1.15 eV for the Mn/W system. This reflects the lower strength of Fe–Fe bonds. In the magnetically ordered state, a Fe adatom creates a ferromagnetic defect in the AF Fe/W(100) film. Hence again diffusion is coupled to spin reorientations. For fixed orientations of the magnetic moments, a barrier of 0.3 eV is calculated for Fe hopping on the AF Fe/W(100) film,[10] hence for both Mn and Fe films magnetic ordering leads to a reduction of the diffusion barriers.

3. Vacancy diffusion in nearly complete 2 ML thick Mn/W(100) films

Since the preceding paragraphs have shown that Mn–Mn interactions in the growing second Mn layer play an important role, we consider here the diffusion of a Mn vacancy within a nearly complete 2 ML thick Mn/W(100) film. Our tests show that at such high concentration the adsorption in hollow sites is preferred, in agreement with the previous results.

Figure 7 summarizes the calculated diffusion barriers. Compared to those calculated for an isolated Mn adatom diffusing on 1 ML Mn/W(100) in magnetic calculations (Fig. 5), for a nearly complete second layer they are found to be typically higher by about 1 eV. This is explained by the larger friction felt by Mn atoms as the consequence of the higher coordination numbers. Similar trends are obtained in nonmagnetic calculations, with much higher diffusion barriers.

B. Diffusion of Mn on Mn/W(110) films

The diffusion of Mn adatoms on Mn/W(110) films leads to a very complex scenario since in paper I we have shown

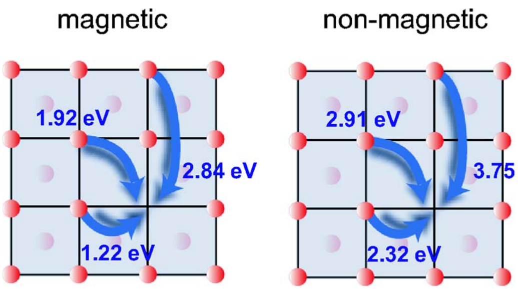

FIG. 7. (Color online) Energetic barriers (in eV) involved in the diffusion of a Mn vacancy in a nearly complete 2 ML thick Mn film adsorbed on the W(100) substrate, in magnetic (left-hand side) or nonmagnetic (right-hand side) calculations.

that in this case a $c(2\times2)$ in-plane antiferromagnetic (AF) order is stabilized. Hence interesting effects resulting from frustration effects due to the magnetic interaction of the adatom with the AF underlayer are to be expected.

1. Adsorption sites

First, like in the preceding section we focus on nonmagnetic calculations. On a nonmagnetic 1 ML thick Mn/W(110) film a Mn adatom adsorbs at a long bridge site; as illustrated in Fig. 8(a) it locally leads to a substantial modification of the local geometry in pushing the first neighboring surface Mn atoms away, so that the Mn adatom is located at only 0.9 Å above the surface. Actually, this configuration turns out to be unstable against the burying of the Mn adatom into the Mn overlayer, the final geometry [see Fig. 8(b)] is almost two dimensional with a dimer incorporated in the surface and a buckling amplitude of 0.3 Å, and is slightly more stable by 0.06 eV. It is very similar to that obtained previously[10] in the system Fe/W. Such a geometry probably allows to relieve locally the large lattice strain resulting from the epitaxial matching of a nonmagnetic Mn overlayer to the W(110) substrate. This can be considered as the first step towards the formation of a locally close-packed capping Mn layer.

On the other hand, for a magnetically ordered AF Mn/W(110) monolayer, the configuration with a Mn atom adsorbed at the same long bridge is stabilized [see Fig. 4(b)], the distortion of the surface is significantly smaller, the adatom is now located 1.6 Å above the surface. It sustains a very large magnetic moment of $4.07\mu_B$ and couples antiferromagnetically with the two first-neighboring surface Mn atoms in agreement with the $c(2\times2)$ in-plane AF order predicted for 2 ML thick films.[8] Even if the magnetic moments of the neighboring Mn atoms are substantially reduced by almost $1\mu_B$, the AF order within the Mn underlayer is not changed. Therefore, the magnetovolume expansion of the Mn ML appears to be the key to the stabilization of the pseudomorphic growth of Mn on W(110).

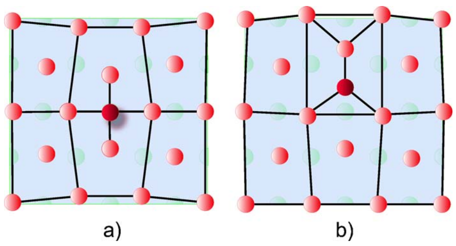

FIG. 8. (Color online) Adsorption of a Mn atom on a 1 ML thick Mn/W(110) film (left-hand side) and further incorporation into the Mn film (right-hand side), as obtained in nonmagnetic calculations.

2. Diffusion barriers

To move from this stable adsorption site to a nearby vacant one, the Mn adatom must jump through a bridge position formed by two nearest-neighboring atoms along the ⟨111⟩ direction. In the transition state, the Mn adatom occupies a short-bridge site. Since the deposition of the Mn adatom does not change the $c(2\times2)$ in-plane AF order of the 1 ML thick Mn underlayer significantly, the two surface Mn atoms involved in the bridge carry large moments of opposite orientation. This leads naturally to a strong frustration effect and in the transition state depicted in Fig. 4(d), the magnetic moment of the Mn adatom is completely quenched, those of the two surface Mn atoms bonding to the adatom are strongly reduced to $\pm1.53\mu_B$. This configuration is energetically very unfavorable, therefore the barrier associated to the Mn adatom hopping is quite high, 1.11 eV, this value is even 2.7 times higher than for the same process on the clean W(110) substrate. This is in evident contrast to our results for the (100) surface where we had found that the barrier for hopping is much lower on the Mn/W(100) ML than on the clean W(100) substrate. The reason is that on the FM Mn/W(100) monolayer no similar frustration effect can occur.

The quenching of the magnetic moment of the Mn adatom in the transition state might be considered as an indication that the magnetic frustration could be released by a canting of the Mn spins. However, due to the symmetry of the transition state ($C_{2v}-2$ mm), only a spin-flop geometry (with a perpendicular orientation of the adatom moment relative to the substrate magnetization) is permitted. Very recently such a spin-flop phase was found to be the ground state of an antiferromagnetic Mn film on a Fe(100).[3,21] The energy gain due to spin-flop ordering relative to the collinear phase was 75 meV upon full relaxation of all geometric and magnetic degrees of freedom. A comparable energy difference may be expected in the present case—this is however one order of magnitude smaller than the difference in the activation energy of the hopping process in the ⟨111⟩ and ⟨100⟩ directions (cf. below). In view of this rather large difference, it is interesting to examine the shape of the potential energy surface in the vicinity of the transition state. A vibrational analysis confirms that the transition state along the ⟨111⟩ direction is a true transition state (only one imaginary mode), but the barrier separating the saddle point from the energetically most favorable transition state is very low.

The antiferromagnetic $c(2\times2)$ structure of 1 ML Mn/W(110) consists of rows of ferromagnetically aligned atoms extending along the ⟨100⟩ and ⟨110⟩ directions, while along the ⟨111⟩ directions up and down spins alternate. No magnetic frustration exists for a hopping in the ⟨100⟩ direc-

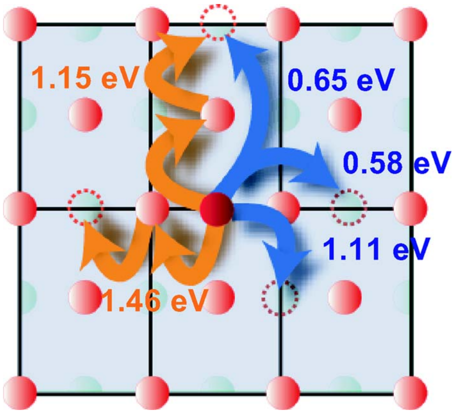

FIG. 9. (Color online) Energetic barriers (in eV) involved in the diffusion of a Mn atom adsorbed on a 1 ML Mn/W(110) film, as obtained in magnetic calculations.

tion to a next-nearest-neighbor bridge position across an on-top transition state. In this case the magnetic coupling of the adatom with the bonding substrate atoms remains AF all along the diffusion path, in the transition state the adatom has a very high magnetic moment of $4.05\mu_B$ [see Fig. 4(e)] coupled antiferromagnetically to the substrate atom below. The absence of frustration results in a low diffusion barrier of 0.58 eV. For a jump over a distance of $a\cdot\sqrt{2}$ along the $\langle 110\rangle$ direction the situation is again different: if no spin-reorientation takes place during the hopping, the moments of the adatom and of the underlying substrate atom are ferromagnetically aligned in the transition state. Hence for hopping in this direction the FM-AF magnetic energy difference adds to the barrier calculated for hopping along $\langle 100\rangle$ if no spin-reorientation takes place during the process. However, in this transition-state configuration, the magnetic energy is small (only 66 meV), together we calculate an activation energy for diffusion of 0.65 eV (see also Fig. 9). For a spin reorientation during the hopping process we expect a similar activation energy. Hence the magnetically broken symmetry leads to a modest anisotropy of hopping diffusion along the $\langle 100\rangle$ and $\langle 110\rangle$ directions.

The rule that magnetic ordering lowers the diffusion barriers is also verified for the exchange processes for which we find much lower energy barriers (1.15 and 1.46 eV) than for Mn adsorbed on the clean W(110) (4.22 and 3.07 eV). But one can observe that the barrier for the exchange along $\langle 100\rangle$ (1.46 eV) is higher than that for the exchange along $\langle 110\rangle$ (1.15 eV), in disagreement with the elastic arguments already mentioned for diffusion on the clean substrate. The reason is that for an exchange process along $\langle 100\rangle$ the transition state consists of a dimer of Mn atoms with antiparallel spin, both atoms must flip their spins to accommodate with the magnetic order of the final state. For an exchange along $\langle 110\rangle$ the atoms in the transition-state dimer have parallel moments and the magnetic order is preserved without any spin reorientation. Hence for hopping and exchange processes, magnetic effects act in opposite directions. All these results demonstrate that magnetic effects like frustration or spin flipping required during the migration processes may have a strong influence on the diffusion properties. As frustration and exchange interactions inducing spin orientations are local effects, the magnetic effects on diffusion will not completely disappear in the paramagnetic phase, as long as short-range correlations between the paramagnetic moments exist.

V. CONCLUSIONS AND OUTLOOK

We have presented an extended first-principles DFT investigation of the elementary dynamical processes occurring during the growth of Mn films on W substrates. Our calculations provide a good picture of the diffusion mechanisms on flat terraces and islands—diffusion across or along step-edges have been excluded for the moment. Both on clean and Mn-covered W-surfaces Mn adatoms diffuse by hopping, while exchange with surface atoms in the underlying layer is strongly disfavored by much higher activation energies. Both hopping and exchange processes are easier on Mn capping layers as a result of the less strong Mn–Mn bonds compared to Mn-W and W–W ones, which stresses the interest of W substrates to generate high-quality magnetic films without significant interdiffusion at the interface.

Spin-polarization turns out to have a very important role in determining the stable adsorption sites and the diffusion properties, even on clean W films. A Mn atom impinging on the tungsten substrate carries a large magnetic moment of $5\mu_B$. The magnetic moment of adsorbed Mn atoms depends on the number of bonds formed with surface atoms and on the distance from the surface. Mn atoms in transition-state configurations have magnetic moments that are about $1\mu_B$ larger than atoms in their stable adsorption sites. Therefore, non-spin-polarized calculations produce much too large diffusion barriers.

On nonmagnetic Mn films on W(100) the preferred adsorption sites for Mn adatoms show a transition from bridge to hollow sites with increasing Mn coverage; this finally stabilizes the pseudomorphic growth at full coverage. On ferromagnetic films, Mn adsorption in the hollow is preferred at all coverages. Different adsorption geometries also lead to different transition state for both hopping and exchange diffusion. For a Mn adatom on Mn/W(110) an even more dramatic effect is found, nonmagnetic Mn/W(110) are under large tensile strain, and as already found for Fe/W(110) films,[10] the adatom forms a buried dimer with a surface atom as a first step towards the formation of a close-packed Mn island. On the other hand, pseudomorphic growth is stabilized if magnetism is taken into account.

For the diffusion properties, the most remarkable effect of magnetism is a general reduction of the activation energies, both for hopping and exchange events. In magnetic calculations, the adatoms are usually located at a larger distance from the substrate than in nonmagnetic ones, and thus see a flatter surface. Due to exchange interactions between adatom and substrate, the scenario for hopping processes becomes much more complex. (i) The magnetic moment of the diffusing atom in its transition state can either be enhanced due to a reduced coordination, or quenched because of local frustrations. (ii) In addition, transient spin-flips of the diffusing atom can reduce the activation energy. The magnetic effects on the diffusion barriers depend on local interactions—hence spin-polarization effects will also be present in the paramagnetic phase, as long as short-range correlations between the paramagnetic moments exist. It would certainly be very interesting to test the predicted magnetic effects by experimental investigations—the calculated differences in the activation energies should be large enough.

However, the modest anisotropies found for Mn diffusion on Mn/W(110) films are certainly not strong enough to explain the observed growth anisotropy. Therefore, another mechanism should be assumed to explain the anisotropy observed experimentally for the W(110) substrate. Extended calculations on stepped surfaces modeling the perimeter of a large island are currently in progress and should clarify this point.

ACKNOWLEDGMENTS

This work has been supported by the EU Commission within the STREP Project "Dynamics in Nano-Scale Materials" (Contract No. NMP4-CT-2003-001516). The calculations were performed on Schrödinger II computer system at the Computer Center of Vienna University.

---

*Electronic address: samuel.dennler@univie.ac.at

[1] D. Hobbs, J. Hafner, and D. Spišák, Phys. Rev. B **68**, 014407 (2003).

[2] J. Hafner and D. Hobbs, Phys. Rev. B **68**, 014408 (2003).

[3] J. Hafner and D. Spišák, Phys. Rev. B **72**, 144420 (2005).

[4] M. Bode, M. Hennefarth, D. Haude, M. Getzlaff, and R. Wiesendager, Surf. Sci. **432**, 8 (1999).

[5] S. Heinze, M. Bode, A. Kubetzka, O. Pietzsch, X. Nie, S. Blügel, and R. Wiesendanger, Science **288**, 1805 (2000).

[6] M. Bode, S. Heinze, A. Kubetzka, O. Pietzsch, M. Hennefarth, M. Getzlaff, R. Wiesendanger, X. Nie, G. Bihlmayer, and S. Blügel, Phys. Rev. B **66**, 014425 (2002).

[7] Y. Tian and F. Jona, J. Phys.: Condens. Matter **13**, 1805 (2001).

[8] S. Dennler and J. Hafner, preceding paper, Phys. Rev. B **72**, 214413 (2005).

[9] M. Aldén, H. L. Skriver, S. Mirbt, and B. Johansson, Surf. Sci. **315**, 157 (1994).

[10] D. Spišák and J. Hafner, Phys. Rev. B **70**, 195426 (2004).

[11] G. Kresse and J. Hafner, Phys. Rev. B **47**, R558 (1993).

[12] G. Kresse and J. Furthmüller, Phys. Rev. B **54**, 11 169 (1996); Comput. Mater. Sci. **6**, 15 (1996).

[13] P. E. Blöchl, Phys. Rev. B **50**, 17 953 (1994).

[14] G. Kresse and D. Joubert, Phys. Rev. B **59**, 1758 (1999).

[15] G. L. Kellog, Surf. Sci. Rep. **21**, 1 (1994).

[16] D. W. Basset and P. R. Webber, Surf. Sci. **70**, 520 (1978).

[17] C. M. Chang, C. M. Wei, and J. Hafner, J. Phys.: Condens. Matter **13**, L321 (2001).

[18] C. M. Chang and C. M. Wei, Chin. J. Phys. (Taipei) **43**, 169 (2005).

[19] G. Henkelman and H. Jónsson, J. Chem. Phys. **111**, 7010 (1999).

[20] M. S. Altman, P. J. Estrup, and I. K. Robinson, Phys. Rev. B **38**, 5211 (1988).

[21] C. Grazioli, D. Alfe, S. R. Krishnakumar, S. S. Gupta, M. Veronese, S. Turchini, N. Bonini, A. Dal Corso, D. D. Sarma, S. Baroni, and C. Carbone, Phys. Rev. Lett. **95**, 117201 (2005).